Since January 2020 Elsevier has created a COVID-19 resource centre with free information in English and Mandarin on the novel coronavirus COVID-19. The COVID-19 resource centre is hosted on Elsevier Connect, the company's public news and information website.

Sensors International 2 (2021) 100131

Contents lists available at ScienceDirect

Sensors International

journal homepage: www.keaipublishing.com/en/journals/sensors-international

Optimal control for COVID-19 pandemic with quarantine and antiviral therapy

Md. Abdullah Bin Masud, Mostak Ahmed *, Md. Habibur Rahman

Department of Mathematics, Jagannath University, Dhaka, 1100, Bangladesh

ARTICLE INFO

MSC:
34A12
49K15
92B05

Keywords:
COVID-19
Optimal control
Pontryagin's maximum principle
Hamiltonian
Transversality conditions

ABSTRACT

In the absence of a proper cure for the disease, the recent pandemic caused by COVID-19 has been focused on isolation strategies and government measures to control the disease, such as lockdown, media coverage, and improve public hygiene. Mathematical models can help when these intervention mechanisms find some optimal strategies for controlling the spread of such diseases. We propose a set of nonlinear dynamic systems with optimal strategy including practical measures to limit the spread of the virus and to diagnose and isolate infected people while maintaining consciousness for citizens. We have used Pontryagin's maximum principle and solved our system by the finite difference method. In the end, several numerical simulations have been executed to verify the proposed model using Matlab. Also, we pursued the resilience of the parameters of control of the nonlinear dynamic systems, so that we can easily handle the pandemic situation.

1. Introduction

Coronavirus is leading to an ongoing pandemic and spread worldwide. If the infected person is in close contact with others, it may cause the COVID-19 virus to spread. The tiny droplets and aerosols carrying the virus can spread from the nose and mouth of an infected person to shortness of breath, coughing, sneezing, singing or talking. If the virus enters their mouth, nose or eyes, then they will be infected. The virus can also spread through contaminated surfaces, although it is not considered the main route of infection. The exact route of infection is rarely proven, when people are close to each other, the infection mainly occurs for a long time. It spreads from infected people who had no symptoms two days before the start of symptoms.

In April 2020, the World Health Organization (WHO) provided detailed information and advisories in its report [1]. A mathematical model is a factual tool to understand how to transmit COVID-19 and exploring different scenarios. The susceptible-infected-recovered (SIR) model is discussed in the Oxford model [2], where data comes from the UK and Italy, and the data relates to the death of the SARS-Cove-2. In that time the Imperial model is discussed against several cumulative deaths in the UK or the US [3]. In Ref. [4], discuss how to spread and develop a model. The rate of spread of this disease is proportional to the multiplication of the numbers of attacked and non-attacked individuals. In Refs. [5,6], researchers proposed a system of differential equations with five different variables: susceptible (S), exposed (E), symptomatic infected (I), asymptomatic infected (A), removed (R) including recovered and dead individuals. Coronavirus is spreading in mass people rapidly, however several vaccines have been developed.

Many countries have already initiated widespread vaccination campaigns to control the disease. Control of coronavirus spread also depends on Quarantine (Q) or Isolation. In Ref. [7], Anwar Zeb et al. improved a quarantine model with four variables SEIR (Susceptible, Exposed, Infected and Recovered). Due to the severity of the COVID-19 pandemic, the necessity of scientific modeling is increasing more. A model can help create a treatment plan and be able to see the long-term course of the pandemic. In Ref. [8], the authors formulated a mathematical model with isolation class and government interference systems to reduce disease infection. And also formulated an optimal control problem. Since the characteristics and ruin of COVID-19 depend on various parameters (such as personal immunity, so a COVID-19 pandemic-infected system

* Corresponding author.
E-mail address: mostak@math.jnu.ac.bd (M. Ahmed).

Production and hosting by Elsevier

https://doi.org/10.1016/j.sintl.2021.100131
Received 9 August 2021; Received in revised form 9 October 2021; Accepted 10 October 2021
Available online 22 October 2021

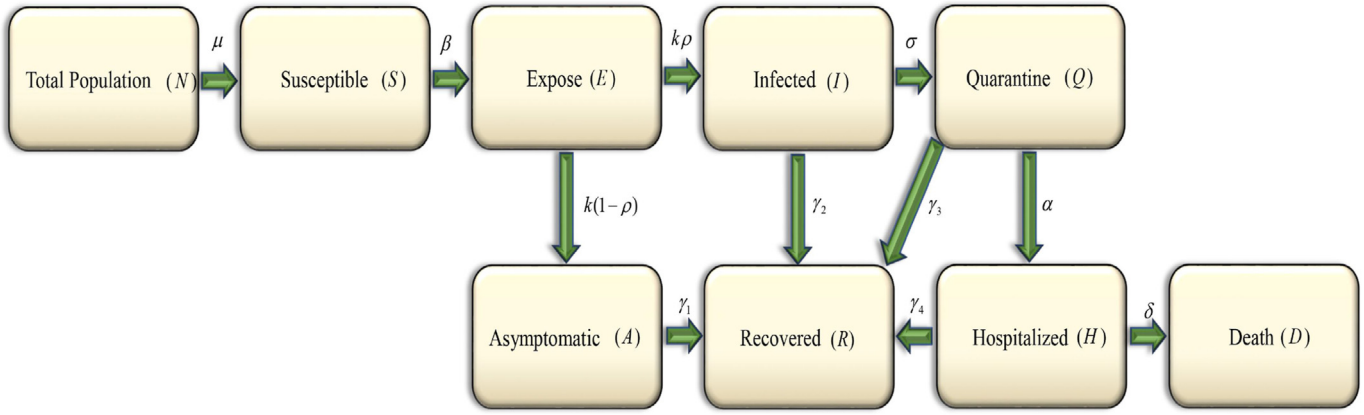

Fig. 1. Schematic diagram of the proposed disease dynamics for COVID-19 pandemic.

has a history of going to the country while maintaining the necessary hygiene), that's why all over the world, we can not describe the whole disease system using a single model. The mathematical model is more accurate but complex when all parameters and complexity are used.

Currently, many mathematical models have been developed to explain COVID-19 transmission. Some recent mathematical models can be found in Refs. [9–12]. In Ref. [11], the authors discussed five compartments (SEIQR) where the natural birth and death rates are the same for the mathematical model is based in India. Furthermore, they discussed the sensitivity of the model on the transmission rate and the rate of recovery. In Ref. [12], the authors discussed two types of susceptibility (non-quarantined and quarantined susceptible populations) in the SIR model and also investigated the impact of the spread of the infection of COVID-19 in Bangladesh. In Ref. [13], the authors described a susceptible-exposed-infectious-recovered metapopulation model with simulating the pandemic across all major parameters and estimated the reproduction number by using Markov Chain Monte Carlo methods. In Ref. [10], the authors describe the three compartmental models with the stability of Hyers-Ulam type and numerical simulated by Adams–Bashforth method. In Ref. [14], the authors introduced nonlinear ordinary equations, analyzed the stability for disease-free and discussed preventive measures, future outbreaks, and potential disease control strategies. In Ref. [15] the authors discuss how India is working with COVID-19 on the economy, human life, and the environment. Social distance and lockdown are good but mitigation of COVID-19 without proper vaccination is a big challenge. Most researchers solve problems without considering the idea of optimal control. We suggest that optimal controls can be used to investigate the effects of antiviral therapy and isolation strategies during pandemics.

In the present study, we propose a mathematical model with control according to our social status which is more challenging. The main objective of this study is to analyze government strategies for control of COVID-19 such as isolation, lockdown, quarantine, etc. Our proposed method can find optimal strategies that reduce infectious and hospitalized patients in a short period [0, T]. We study the completely dynamic behavior of the model in terms of basic reproduction numbers. We have used three control variables $u_1(t)$, $u_2(t)$ and $u_3(t)$, where.

- $u_1(t)$ is the antiviral therapy control on clinically infected cases,
- $u_2(t)$ is the antiviral therapy control on hospitalizations, and
- $u_3(t)$ is the isolation control on hospitalizations.

Our aim is to determine the optimal solution of control variables. Combining antiviral and isolation, we searched for results for a single policy or multiple policies. Finally, we analyze the sensitivity of the required parameters.

2. Preliminary results

The formation of a model is a mathematical representation of a natural system. Several mathematical models are well-established to represent the dynamics of disease. Before constructing a mathematical model for COVID-19, we would like to introduce some basic concepts as well as some established models.

2.1. SIR model

SIR (Susceptible, Infected and Recovered) is more vogue and a basic model is extensively used in the analysis of the expansion of the disease. The time-variant SIR models have been used to calculate the parameters of infection and the number of reproductions [16]. There are three classes in the SIR model, known as susceptible or susceptive or sensitive, contagious, or Infectious and recovered. Non-infectious populations become susceptible and the whole population could become infected with COVID-19 because there is still no vaccine [17]. A man with a sensitive level goes into an infectious level when that man is in or in the vicinity of an infected man [18]. As the disease becomes infectious, the number of infected people continues to increase and people with sensitive levels are more likely to be infected and enter the infection level. For those who are not contagious, the recovered person represents them. The equations of the SIR model have become as follows:

$$\begin{cases} \dfrac{dS(t)}{dt} = -\beta IS \\ \dfrac{dI(t)}{dt} = \beta IS - \gamma I \\ \dfrac{dR(t)}{dt} = \gamma I \end{cases}, \tag{1}$$

where each infected person has a certain number β of contacts per day to spread the disease and γ represents the rate of recovery from infected people.

2.2. SEIR model

In epidemiological studies at the level of population, the SEIR (Susceptible, Exposed, Infected and Recovered) model is one of the most conventional and relatively simple mathematical structures. The SEIR model is an ordinary and comparatively normal mathematical form. The SEIR model consists of four compartments: the susceptible population $S(t)$ at time t; the exposed population $E(t)$; the infected population $I(t)$; the recovered population $R(t)$. In a limited process, the sum $N(t) = S(t) + E(t) + I(t) + R(t)$ of these divisions remains constant over

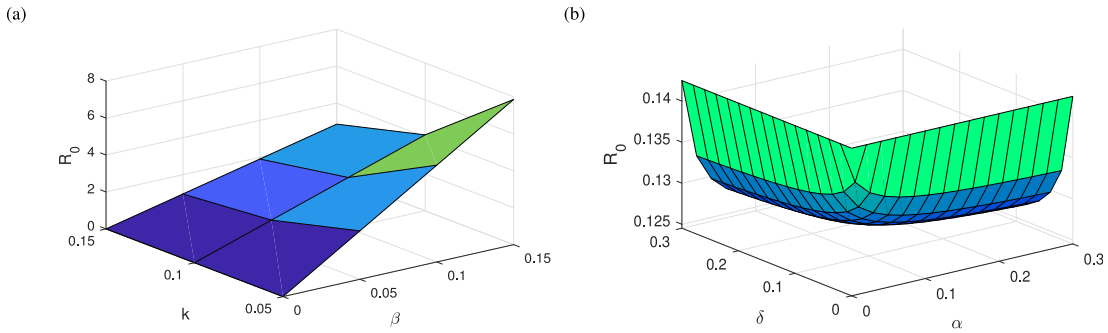

Fig. 2. Effect of parameters in reproduction number: (a) for β-k and (b) for α-δ.

time where birth and death are not responsible. The combined dynamic of these sections is narrated by the method of the equation below:

$$\begin{cases} \dfrac{dS(t)}{dt} = N - \beta S(I+E) \\ \dfrac{dE(t)}{dt} = \beta S(I+E) - kE \\ \dfrac{dI}{dt} = kE - \gamma I \\ \dfrac{dR(t)}{dt} = \gamma I \end{cases}, \tag{2}$$

where k is the rate at which latent individuals become infected.

2.3. The conventional model of COVID-19

We propose a model similar to the influenza pandemic model described in Ref. [19]. For this purpose, we classify individuals as susceptible ($S(t)$), exposed ($E(t)$), clinically ill and infections ($I(t)$), asymptomatic ($A(t)$), quarantine ($Q(t)$), hospitalized ($H(t)$), recovered ($R(t)$) and death ($D(t)$). Fig. 1 is used to form the model of COVID-19 by the following set of nonlinear differential equations:

$$\begin{cases} \dfrac{dS(t)}{dt} = N - \{\mu S + \beta S(E+I+qA+Q+H)\} \\ \dfrac{dE(t)}{dt} = \beta S(I+qA+Q+H) - kE \\ \dfrac{dA(t)}{dt} = k(1-k)\rho E - \gamma_1 A(t) \\ \dfrac{dI(t)}{dt} = k\rho E - (\gamma_2+\sigma)I \\ \dfrac{dQ(t)}{dt} = \sigma I - (\alpha+\gamma_3)Q \\ \dfrac{dH(t)}{dt} = \alpha Q - (\gamma_4+\delta)H \\ \dfrac{dR(t)}{dt} = \gamma_1 A + \gamma_2 I + \gamma_3 Q + \gamma_4 H \\ \dfrac{dD(t)}{dt} = \delta H \end{cases} \tag{3}$$

where $N(t) = S(t) + E(t) + I(t) + A(t) + Q(t) + H(t) + R(t)$ is the total population at time t. $\rho(0 < \rho < 1)$ is the constant ratio of exposed $E(t)$ at growth rate k to the clinically infectious sector $I(t)$ while the remaining $(1-\rho)k$ comes from $E(t)$ to the in part of asymptomatic sector $A(t)$. The γ_1, γ_2, γ_3 and γ_4 are the rate of recovered from the sectors symptomatic, infected, quarantine and hospitalization respectively. The constants α and δ are the hospitalized rate which comes from quarantine and the death rate which comes from hospitalization.

2.4. Basic reproduction number

In epidemiology, $\mathcal{R}_0$ is the basic reproduction number of an infection which is the expected number of a class directly generated susceptible to infection in a population [23,24]. $\mathcal{R}_0$ is not an original constant for any virus due to being influenced by other factors such as the conditions of the environment and the attitude of infected populations. The values of $\mathcal{R}_0$ are normally inferred from mathematical models and the approximate values depend on the use of parameters and the other parameters values.

According to Ref. [25], the formation of $\mathcal{R}_0$ and threshold parameters from deterministic as well as a non-deterministic model are discussed. In that article, the authors consider a next-generation matrix $G = FV^{-1}$. According to our model,

$$\mathcal{F} = \begin{bmatrix} (\mu S + \beta S(E+I+qA+Q+H)) \\ 0 \\ 0 \\ 0 \\ 0 \end{bmatrix}$$

$$\mathcal{V} = [kE - k(1-k)\rho E + \gamma_1 A - k\rho E + (\gamma_2+\sigma)I - \sigma I + (\alpha+\gamma_3)Q - \alpha Q + (\gamma_4+\delta)H]$$

$$F = \begin{bmatrix} \beta & q\beta & \beta & \beta & \beta \\ 0 & 0 & 0 & 0 & 0 \\ 0 & 0 & 0 & 0 & 0 \\ 0 & 0 & 0 & 0 & 0 \\ 0 & 0 & 0 & 0 & 0 \end{bmatrix}$$

$$V = \begin{bmatrix} k0000 - k(1-k)\rho - k\rho & & & & \\ \gamma_1 000 - k\rho - k\rho & & & & \\ & 0 & (\gamma_2+\sigma) & 0 & 0 \\ 0 & 0 & -\sigma & \alpha+\gamma_3 & 0 \\ 0 & 0 & 0 & -\alpha & \gamma_4+\delta \end{bmatrix}$$

$\mathcal{R}_0$ is the dominant eigenvalue of the matrix. The dynamic feature of the model (3) in the lack of control is characterized by the number of basic reproduction numbers $\mathcal{R}_0$, and also $\mathcal{R}_0$ is an assessment of the number of secondary classes formed by infectious classes when acquainted with a fully sensitive population. Without controls $u_i(t) = 0$, $i = 1, 2, 3$,

$$\mathcal{R}_0 = \frac{\beta}{k\gamma_1}(1+q(1-k)) + \beta\rho \times \left\{ \frac{1}{(\gamma_2+\sigma)} \left(1 + \frac{\sigma}{(\gamma_3+\alpha)} + \frac{\sigma\alpha}{(\gamma_3+\alpha)(\gamma_3+\delta)} \right) \right\} \tag{4}$$

is the reproduction number of the model (3). In Fig. 2(a), R_0 is increased when β is increased but R_0 is decreased when k is decreased. In Fig. 2(b),

Table 1
Parameter values with description.

Parameter list			
Parameter	Description	Value or range	Reference
$N(t)$	Total Population	18 crores	Proposed
$S(0)$	Susceptible at time $t = 0$	13 crores	Proposed
$E(0)$	Exposed at time $t = 0$	3 crores	Proposed
$A(0)$	Asymptomatic at time $t = 0$	0	
$I(0)$	Initially Infectious	0	
$Q(0)$	Initially Quarantined	0	
$H(0)$	Initially Hospitalized	0	
$R(0)$	Initially Recovered	0	
μ	Transmission rate from N (day^{-1})	0.02[0.01-1.25]	[20]
β	Exposed rate from Susceptible ($days^{-1}$)	0.01[0.001-2.5]	[21]
q	Relative infectiousness of the asymptomatic class	0.03	Proposed
k	Clinical Infectious rate ($days^{-1}$)	0.01	Proposed
ρ	Constant Proportion of latent individuals	0.01	Proposed
σ	Isolated rate ($days^{-1}$)	0.3	Proposed
α	Hospitalized rate ($days^{-1}$)	0.07	Proposed
γ_1	Recovered class rate from Asymptomatic	0.02	Proposed
γ_2	Recovered rate from Infectious ($days^{-1}$)	0.02	Proposed
γ_3	Recovered rate from Quarantine ($days^{-1}$)	0.02	Proposed
γ_4	Recovered rate from Hospital ($days^{-1}$)	0.02	Proposed
δ	The death rate from Hospital ($days^{-1}$)	0.01	[22]

R_0 is decreased when α and δ are decreased.

In the next section we are going to introduce three controls in the parameterized model for COVID-19 transmission are included in the system of the nonlinear differential equation (3).

3. Model of COVID-19 pandemic with control

Based on data from the COVID-19 pandemic around the world, the optimal control theory is used to explore the effects of antiviral therapy and isolation strategies on modeling parametrized scenes. The control functions $u_i(t)$, $i = 1, 2, 3$, where $u_1(t)$ is clinical infectious control; $u_2(t)$ and $u_3(t)$ are the hospitalization control formulated by the different policies. The dynamics of disease are modeled with control by the following set of nonlinear differential equations

$$\begin{cases} \frac{dS(t)}{dt} = \mu N - \{\mu S + \beta S(E + I + qA + Q + (1 - \varepsilon_3 u_3(t))H)\} \\ \frac{dE(t)}{dt} = \beta S(I + qA + Q + (1 - \varepsilon_3 u_3(t))H) - kE \\ \frac{dA(t)}{dt} = k(1 - k)\rho E - \gamma_1 A(t) \\ \frac{dI(t)}{dt} = k\rho E - (\gamma_2 + \sigma + \varepsilon_1 u_1(t))I \\ \frac{dQ(t)}{dt} = \sigma I - (\alpha + \gamma_3)Q \\ \frac{dH(t)}{dt} = \alpha Q - (\gamma_4 + \delta + \varepsilon_2 u_2(t))H \\ \frac{dR(t)}{dt} = \gamma_1 A + \gamma_2 I + \gamma_3 Q + \gamma_4 H + \varepsilon_1 u_1(t)I + \varepsilon_2 u_2(t)H \\ \frac{dD(t)}{dt} = \delta H. \end{cases} \tag{5}$$

The Lebesque Integrable functions $u_i(t)$, $i = 1, 2, 3$ are bounded in [0, 1]. Control attempts $u_1(t)$ model the fraction of infectious class treated with antivirals per unit of clinical time, while control $u_2(t)$ model the fraction of patients receiving antiviral therapy per unit of time hospitalized. We assume that both controls have uninterrupted antiviral competence $\varepsilon_1 = \varepsilon_2$, incorporated in the model as $\varepsilon_1 u_1(t)$ and $\varepsilon_2 u_2(t)$. $(1 - \varepsilon_3 u_3(t))H(t)$ is the isolation control, which is prevented the interactions between $H(t)$ and $S(t)$ classes; and the competence constant ε_3 is the impact of isolation in hospital. Control variables close to 1 ($u_1(t) \approx 1$ and $u_2(t) \approx 1$) represent almost complete effort and the situation of the model in almost every infectious or hospitalized person receiving antiviral therapy. If communication between sensitive and hospitalized people is almost completely avoided and is prevented by effective isolation, then $\varepsilon_3 u_3(t) \approx 1$. The competence of controls $u_i(t)$ are modified by changing the competence constant ε_i ($i = 1, 2, 3$). It should be noted that for numerical computation, values of parameters will be used from Table 1.

4. Main result

In an optimization problem, the objective function F is used to optimize, where the admissible sets ($u_1(t)$, $u_2(t)$, $u_3(t)$) are identifying the most effective strategies over a finite time interval. The goal is to reduce the number of clinically infectious and hospitalized patients in the final period of time at a minimal cost. The function

$$F(u_1(t), u_2(t), u_3(t)) = \int_0^T \left[C_1 I(t) + C_2 Q(t) + C_3 H(t) + \frac{W_1}{2} u_1^2(t) + \frac{W_2}{2} u_2^2(t) + \frac{W_3}{2} u_3^2(t) \right] dt \tag{6}$$

is the objective function of the system of equation (5) which is minimized.

The control efforts are assumed to be nonlinear. We choose to model the control effects using a linear combination of quadratic terms $u_i^2(t)$, $(i = 1,2,3)$, where the coefficients C_i, and the weight constants W_i, ($i = 1, 2, 3$) are pre-selected as a measure of the relative cost of the interference within [0, T]. Since variables of (5) satisfy the initial conditions, then finding optimal functions $u_i^*(t)$, $i = 1, 2, 3$ such that

$$F(u_i^*(t),\ i = 1, 2, 3) = \min_{\Omega} F(u_i(t),\ i = 1, 2, 3), \tag{7}$$

where

$$\Omega = \{(u_1(t), u_2(t), u_3(t)) \in (L^2(0, T))^3 \mid 0 \le u_1(t), u_2(t), u_3(t) \le 1, \quad t \in [0, T]\}. \tag{8}$$

This optimal control problem is solved by Pontryagin's maximum principle. The development of the prerequisites is given below. System (5) along with the objective functional (6) are converted by Pontryagin's maximum principle [26]. In this case the Hamiltonian equation can be written as follows:

$$\begin{aligned} J = \quad & C_1 I(t) + C_2 Q(t) + C_3 H(t) + \frac{W_1}{2} u_1^2(t) + \frac{W_2}{2} u_2^2(t) + \frac{W_3}{2} u_3^2(t) \\ & + \lambda_1(t)\{\mu N - \{\mu S + \beta S(E + I + qA + Q + (1 - \varepsilon_3 u_3(t))H)\}\} \\ & + \lambda_2(t)\{\beta S(I + qA + Q + (1 - \varepsilon_3 u_3(t))H) - kE\} \\ & + \lambda_3(t)\{k(1 - k)\rho E - \gamma_1 A(t)\} \\ & + \lambda_4(t)\{k\rho E - (\gamma_2 + \sigma + \varepsilon_1 u_1(t))I\} \\ & + \lambda_5\{\sigma I - (\alpha + \gamma_3)Q\} \\ & + \lambda_6\{\alpha Q - (\gamma_4 + \delta + \varepsilon_2 u_2(t))H\}. \end{aligned} \tag{9}$$

Theorem 1. *System* (3) *has an unique solution if it satisfies the initial conditions for* $S(0)$, $E(0)$, $A(0)$, $I(0)$, $Q(0)$, $H(0)$, $R(0)$.

Proof. System (3) can be written as

$$\varphi(X) = AX + B(X), \tag{10}$$

where,

$$\varphi(X) = \begin{bmatrix} \frac{dS}{dt} \\ \frac{dE}{dt} \\ \frac{dA}{dt} \\ \frac{dI}{dt} \\ \frac{dQ}{dt} \\ \frac{dH}{dt} \\ \frac{dR}{dt} \end{bmatrix}, \; X = \begin{bmatrix} S \\ E \\ A \\ I \\ Q \\ H \\ R \end{bmatrix},$$

$$A = \begin{bmatrix} -\mu & 0 & 0 & 0 & 0 & 0 & 0 \\ 0 & -k & 0 & 0 & 0 & 0 & 0 \\ 0 & k(1-k)\rho & -\gamma_1 & 0 & 0 & 0 & 0 \\ 0 & k\rho & 0 & -(\gamma_2+\sigma) & 0 & 0 & 0 \\ 0 & 0 & 0 & \sigma & -(\alpha+\gamma_3) & 0 & 0 \\ 0 & 0 & 0 & 0 & \alpha & -(\gamma_4+\delta) & 0 \\ 0 & 0 & \gamma_1 & \gamma_2 & \gamma_3 & \gamma_4 & 0 \end{bmatrix},$$

$$B(X) = \begin{bmatrix} N - \beta S(E + I + qA + Q + H) \\ \beta S(I + qA + Q + H) \\ 0 \\ 0 \\ 0 \\ 0 \\ 0 \end{bmatrix}.$$

The second term on the right-hand side of (10) satisfies

$$\begin{aligned} |B(X_1) - B(X_2)| &= |\beta(S_1E_1 - S_2E_2)| \\ &= |\beta(S_1E_1 - S_2E_1 + S_2E_1 - S_2E_2)| \\ &= |\beta(E_1(S_1 - S_2) + S_2(E_1 - E_2))| \\ &\le \beta(|E_1(S_1 - S_2)| + |S_2(E_1 - E_2)|) \\ &\le \beta(|E_1\|S_1 - S_2| + |S_2\|E_1 - E_2|) \\ &= \frac{\beta^2 z}{\mu}(|S_1 - S_2| + |E_1 - E_2|) \\ &= M|X_1 - X_2| \end{aligned}$$

where $M = \frac{\beta^2 z}{\mu}$, then $\|\varphi(X_1) - \varphi(X_2)\| = V\||X_1 - X_2|$, where $V = \max(M, \|A\|) < \infty$.

Thus, it follows that the function φ is uniformly Lipschitz continuous. From the restriction on $S(t) \ge 0$, $E(t) \ge 0$, $A(t) \ge 0$, $I(t) \ge 0$, $Q(t) \ge 0$, $H(t) \ge 0$ and $R(t) \ge 0$, we see by Ref. [27] that a solution of system (3) exists, which is unique. □

Theorem 2. *If the objective functional* $F(u_1(t), u_2(t), u_3(t))$ *over* Ω *is minimized by the optimal controls* $u_1^*(t), u_2^*(t), u_3^*(t)$ *and corresponding solutions* $S^*, E^*, A^*, I^*, Q^*, H^*, R^*, D^*$, *then there exist continuous functions* $\lambda_i(t)$ *such that*

$$\begin{cases} \frac{d\lambda_1}{dt} = (\lambda_1 - \lambda_2)\beta(I + qA + Q + (1 - \varepsilon_3 u_3)H + \lambda_1(\mu + \beta E) \\ \frac{d\lambda_2}{dt} = \lambda_1\beta S + \lambda_2 k - \lambda_3 k(1-k)\rho - \lambda_4 k\rho \\ \frac{d\lambda_3}{dt} = \lambda_3\gamma_1 + (\lambda_1 - \lambda_2)\beta Sq \\ \frac{d\lambda_4}{dt} = -C_1 + \lambda_4(\gamma_2 + \sigma + \varepsilon_1 u_1) + (\lambda_1 - \lambda_2)\beta S - \lambda_5\sigma \\ \frac{d\lambda_5}{dt} = -C_2 + \beta S(\lambda_1 - \lambda_2) + \lambda_5(\alpha + \gamma_3) - \lambda_6\alpha \\ \frac{d\lambda_6}{dt} = -C_3 + (\lambda_1 - \lambda_2)\beta S(1 - \varepsilon_3 u_3) + \lambda_6(\gamma_4 + \delta + \varepsilon_2 u_2) \end{cases} \tag{11}$$

with the transversality conditions, $\lambda_i(T) = 0$, $i = 1, 2, 3, 4, 5, 6$.

Furthermore,

$$\begin{cases} u_1^*(t) = \min\left\{\max\left\{0, \frac{\lambda_4\varepsilon_1 I}{W_1}\right\}, 1\right\}, \\ u_2^*(t) = \min\left\{\max\left\{0, \frac{\lambda_6\varepsilon_2 H}{W_2}\right\}, 1\right\}, \\ u_3^*(t) = \min\left\{\max\left\{0, \frac{(\lambda_2 - \lambda_1)\varepsilon_3\beta HS}{W_3}\right\}, 1\right\}. \end{cases} \tag{12}$$

Proof. The existence of optimal follows from Corollary 4.1 of [26] since the integrand of J is a convex function of (u_1, u_2, u_3) and the state system satisfies the Lipshitz property concerning the state variables. The following can be derived from Pontryagin's Maximum Principle [26]:

$$\frac{d\lambda_1}{dt} = -\frac{\partial J}{\partial S}, \; \frac{d\lambda_2}{dt} = -\frac{\partial J}{\partial E}, \; \frac{d\lambda_3}{dt} = -\frac{\partial J}{\partial A},$$
$$\frac{d\lambda_4}{dt} = -\frac{\partial J}{\partial I}, \; \frac{d\lambda_5}{dt} = -\frac{\partial J}{\partial Q}, \; \frac{d\lambda_6}{dt} = -\frac{\partial J}{\partial H},$$

with $\lambda_i(T) = 0$, $i = 1, 2, \ldots, 6$ evaluated at the optimal controls and corresponding states, which results in the adjoint system (11). We have to minimize the Hamiltonian J with respect to the controls u_1, u_2, u_3 in the set Ω, which gives the following optimality conditions:

$$\begin{cases} \frac{\partial J}{\partial u_1} = W_1 u_1 - \lambda_4\varepsilon_1 I = 0, \; u_1 = u_1^*, \\ \frac{\partial J}{\partial u_2} = W_2 u_2 - \lambda_6\varepsilon_2 H = 0, \; u_2 = u_2^*, \\ \frac{\partial J}{\partial u_3} = W_3 u_3 + \lambda_1 S\varepsilon_3 H - \lambda_2\varepsilon_3 HS = 0, \; u_3 = u_3^*. \end{cases} \tag{13}$$

From (13), we have

$$\begin{cases} u_1^*(t) = \frac{\lambda_4\varepsilon_1 I}{W_1}, \\ u_2^*(t) = \frac{\lambda_6\varepsilon_2 H}{W_2}, \\ u_3^*(t) = \frac{(\lambda_2 - \lambda_1)\varepsilon_3 HS}{W_3}. \end{cases} \tag{14}$$

5. Numerical results

In this section, we will present some simulation results of our proposed approach that can be helpful for policymakers of a state as well as population awareness. The corresponding basic reproduction number creates the existence and uniqueness of the response to guarantee the solution of the control system for the model of COVID-19. We assess the impact of optimal control strategies on the dynamics of the COVID-19

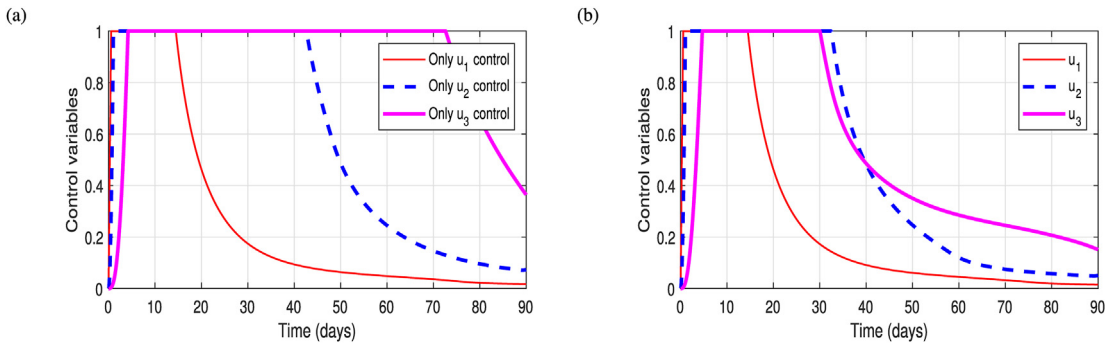

Fig. 3. Effect of controls for the weight constants $W_1 = 0.01$, $W_2 = 0.0007$, $W_3 = 0.0000003$: (a) for the single control and (b) for all controls together.

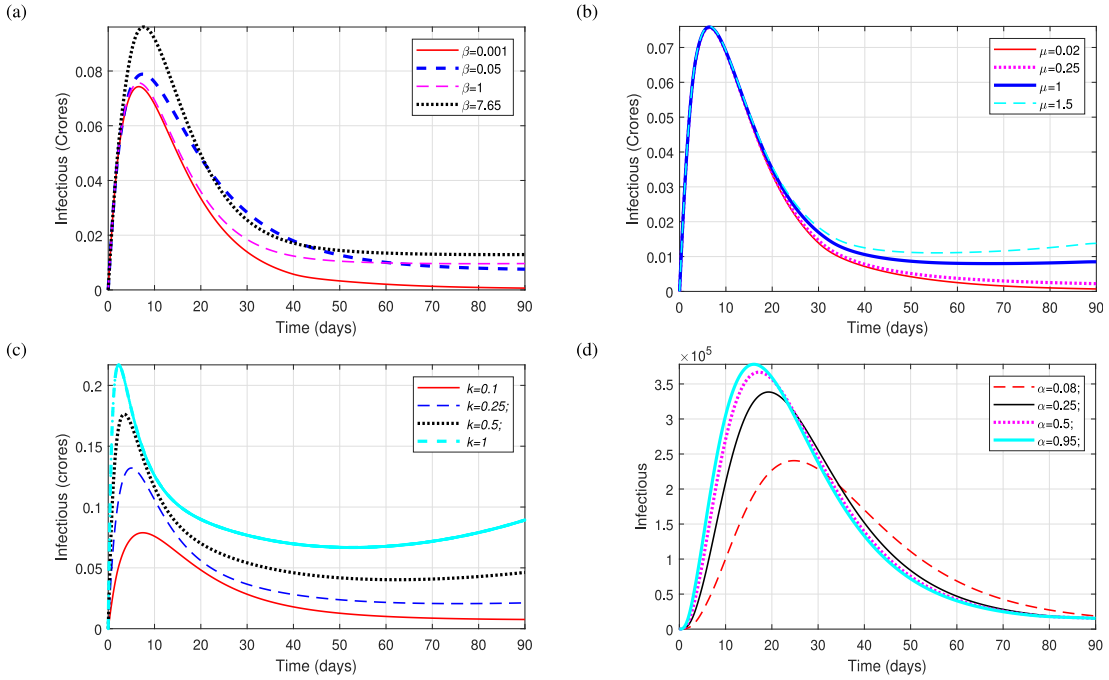

Fig. 4. Effect of parameters: (a) β effect, (b) μ effect, (c) k effect and (d) α effect.

pandemic under the specific baseline reproduction number $\mathcal{R}_0$. As we know, in the case of a pandemic for diseases such as COVID-19, the rational range for the basic reproductive number $\mathcal{R}_0$ should be 1.5–6.49 [28,29]. However, we also check our model for an out-of-range $\mathcal{R}_0$ value and see that the control variables still work. In general, higher reproduction numbers $\mathcal{R}_0 \geq 3.25$ lead to pandemics characterized by high epidemic peaks.

Suppose antiviral drugs have an unlimited supply. The control variables $u_1(t)$, $u_2(t)$ and $u_3(t)$ are applied separately as shown in Fig. 3(a). After a certain period of time, the curve of $u_1(t)$ falls rapidly but the curves of $u_2(t)$ and $u_3(t)$ fall slowly, which ensures that the strategies are not working well. We have shown that the performance of $u_2(t)$ is not so good if antiviral therapy control is applied to hospital admissions but isolation control is not applied to hospital admissions. While three control attempts work simultaneously, it performs better as shown in Fig. 3(b). From Fig. 3, it can be seen that the effect of the control $u_3(t)$ is stronger when we apply all controls together than that of the controls alone. On the other hand, the effect of controls $u_1(t)$ remain close to the same in both cases.

Fig. 4 shows the effect of parameters β, μ, k and α over the population. It can be seen from Fig. 4(a) that $I(t)$ is asymptotically stable when $\beta < 1$ and stable when $\beta \geq 1$. Under full control, the maximal infectivity is 10 days after the onset of the pandemic, and the peak time approximately changes with the transmission rate β. At the peak point near about 8000 infected out of 1,300,000 and after 90 days, the infected is zero when $\beta = 0.001$. The peak date of $I(t)$ is small sensitive to the change of β. Fig. 4(b) shows that $I(t)$ is asymptotically stable at $\mu < 1$, stable at $\mu = 1$, and unstable at $\mu > 1$. Under fully controlled, the maximum number of infected people is at 10th day after starting the pandemic, and the peak time is fixed with the rate of transmission μ. At the peak, 8000 people out of 1,300,000 are infected, and after 90 days, the number of infected is zero when $\mu = 0.02$. The peak date of $I(t)$ is not sensitive to the change of μ.

From Fig. 4(c), it can be seen that $I(t)$ is asymptotically stable for all values of k. Under full control for $k = 1$, the maximum number of infected is at the 8th day after the pandemic starts, and the peak is not fixed while the value of k varies. At the peak level, 7500 (approximate) people are infected out of 1,300,000; after 80 days, the number of infected becomes zero. It is clear that at the peak, $I(t)$ is very sensitive with the change of the value of k. Fig. 4(d) shows that $I(t)$ is asymptotically stable for all values of α. Under full control with $\alpha = 0.08$, the number of the hospitalized patients is maximum on the 23rd day after the start of the pandemic; and the peak varies with the changes in the value of α. At the peak point, 2200 out of 1,300,000 people were hospitalized. The peak of $H(t)$ is sensitive to the change of k.

Fig. 5 shows that the infectious peaks are located at two distinct points for different values of $\mathcal{R}_0$. The pick with full control and only $u_1(t)$

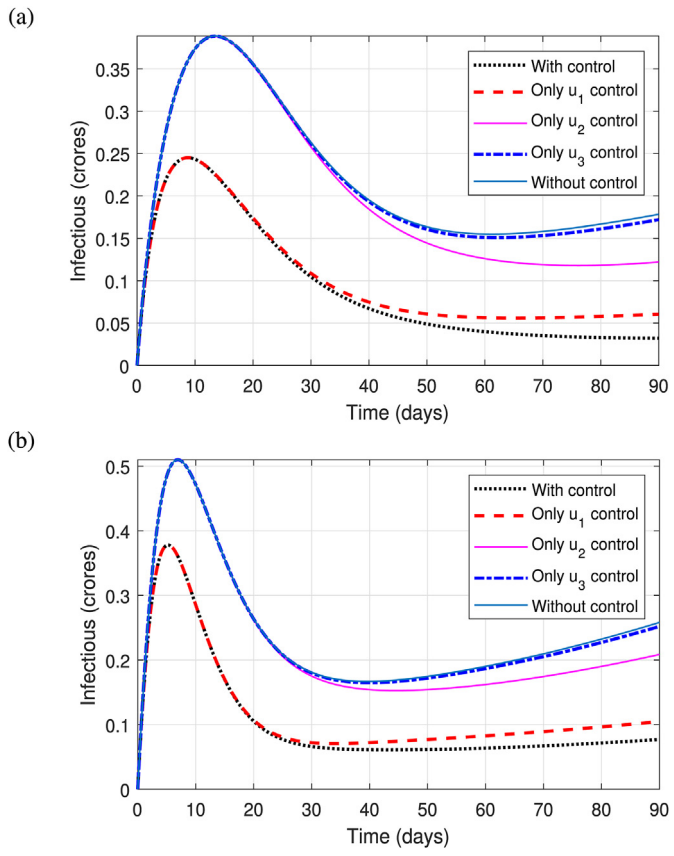

Fig. 5. Symptomatic infected individuals while $\mathcal{R}_0$ and k vary: (a) $\mathcal{R}_0 = 1.47$, k = 0.1, and (b) $\mathcal{R}_0 = 6.65$, k = 0.2.

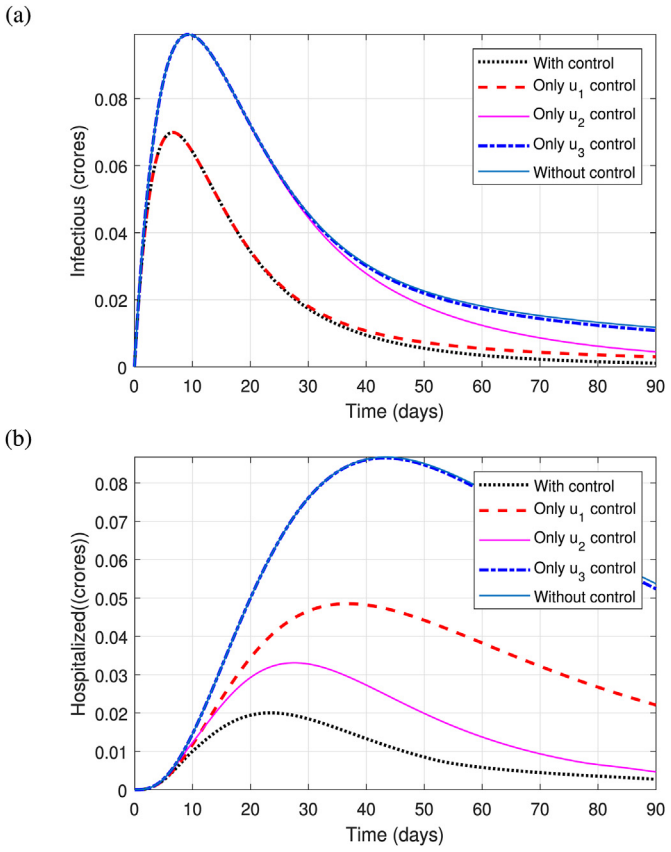

Fig. 8. Comparing control and without control: (a) Infected, and (b) Hospitalized.

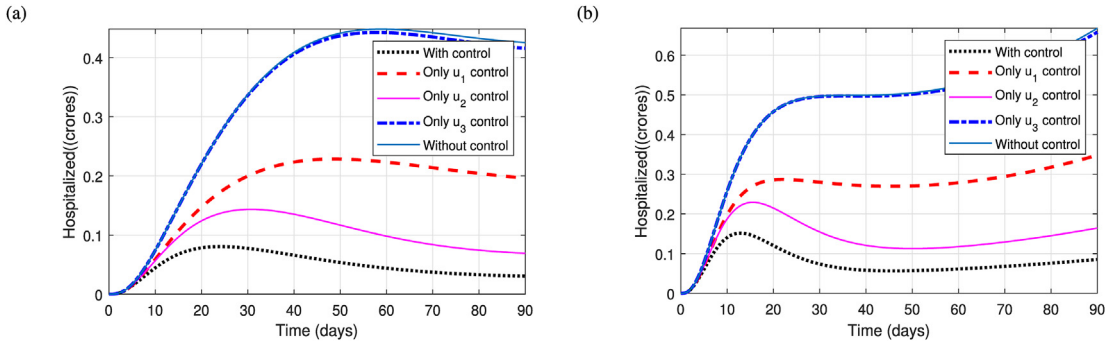

Fig. 6. Number of hospitalized individuals while $\mathcal{R}_0$ and α vary: (a) $\mathcal{R}_0 = 1.47$, $\alpha = 0.3$, and (b) $\mathcal{R}_0 = 6.15$, $\alpha = 0.7$.

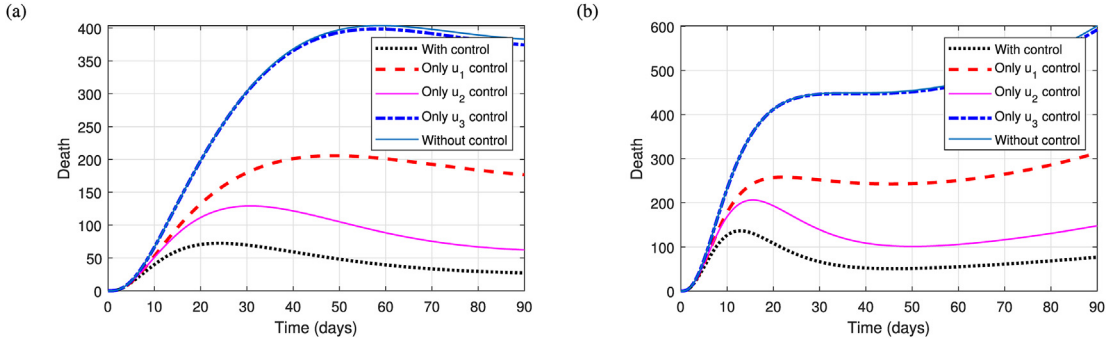

Fig. 7. Number of deaths while $\mathcal{R}_0$ and δ vary: (a) $\mathcal{R}_0 = 1.47$, $\delta = 0.01$, (b) $\mathcal{R}_0 = 6.15$, $\delta = 0.05$.

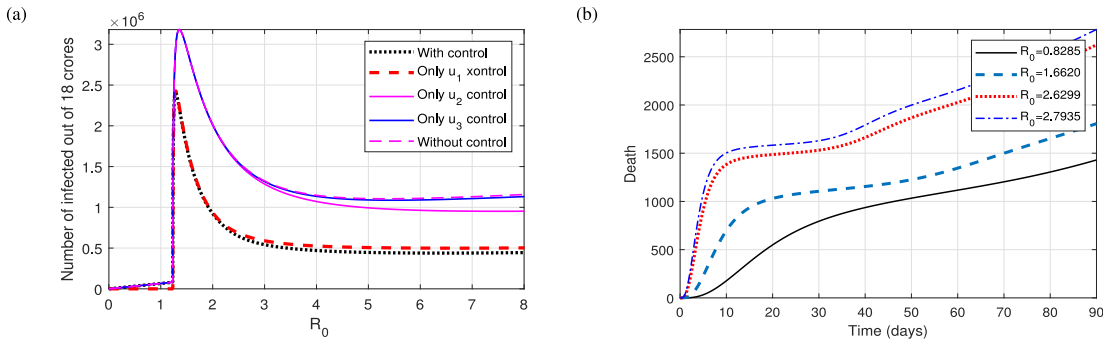

Fig. 9. (a) Infected vs. Reproduction number and (b) Death vs. Time (days).

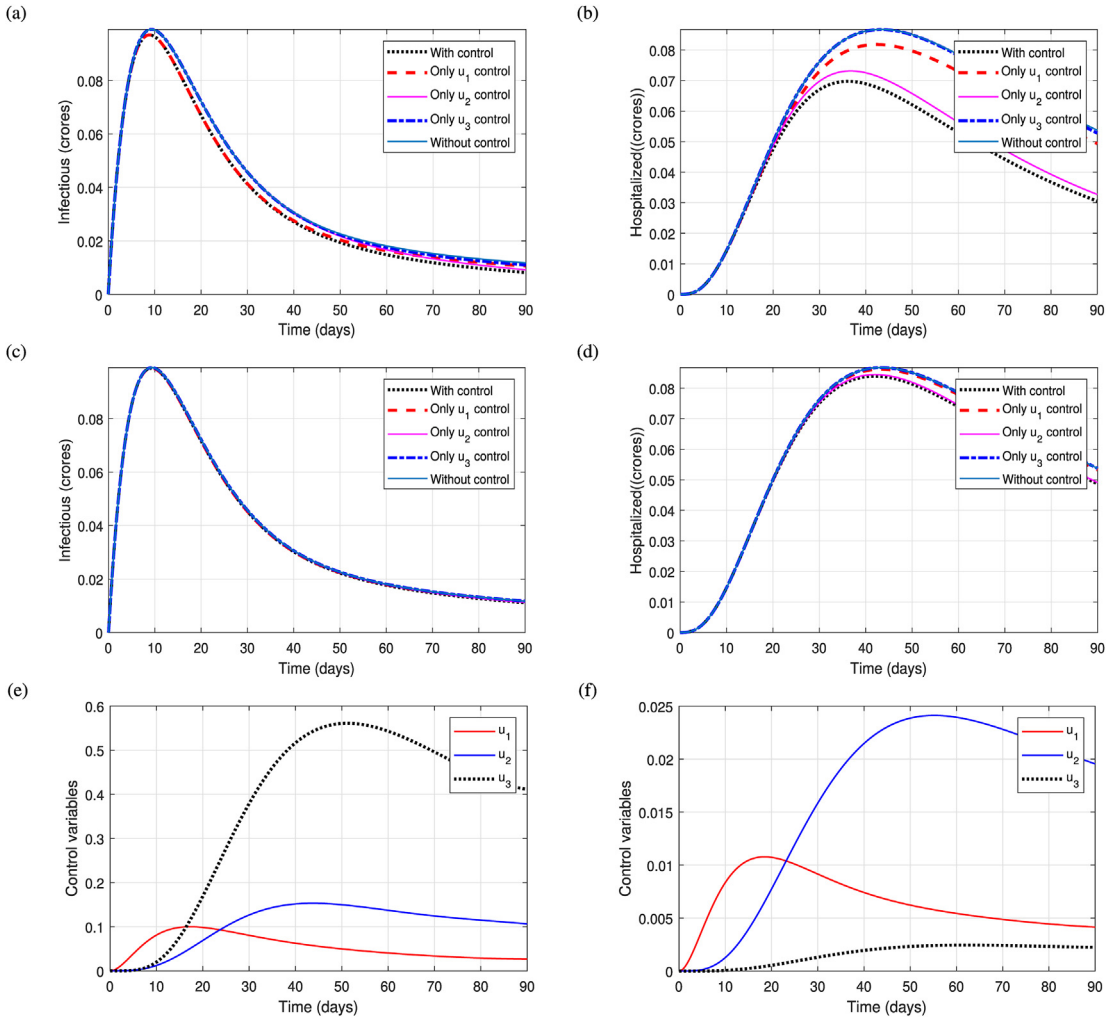

Fig. 10. Comparison of daily infected and hospitalized cases for COVID-19 with relevant control variables. The figures (a,c,e) use weight constants $W_1 = 10$, $W_2 = 10$, $W_3 = 0.03$, and figures (b,d,f) use weight constants $W_1 = 100$, $W_2 = 100$, $W_3 = 10$. Parameter values are given in Table 1.

control are the same. On the other hand, the pick with only $u_2(t)$, $u_3(t)$ controls and without control is the same. It can be observed that the control of antiviral therapy is the most effective only in the case of hospitalizations, except for the control of antiviral therapy and the isolation of hospitalizations alone. With all controls, the rate of infection and hospitalization decreases and stabilizes over time $[0, T]$. In the absence of appropriate vaccination, the isolation strategy is a powerful tool in controlling a pandemic situation. In Fig. 5, the number of symptomatic infected individuals is shown while $\mathcal{R}_0$ and k vary. It can be observed that the number of infected individuals decreases over time when the control variable(s) is imposed. A similar scenario can be seen for the case of hospitalized and dead individuals from Fig. 6 and Fig. 7 correspondingly. It can be seen in Fig. 7 that the number of deaths increases with the increase of reproduction number. Our aim is to minimize the basic reproduction number $\mathcal{R}_0 < 1$ by applying our proposed optimal control strategies.

Fig. 8(a) shows the status of daily infection where $\mathcal{R}_0 = 0.92$. This curves positively skewed distribution shows that the optimal controls are functioning well over the time. On the 8th day, the number of infected is maximum, and after 8th day, the infection rate gradually decreases. The

impact of the controls $u_2(t)$ and $u_3(t)$ are least over the infected people. Fig. 8(b) shows the daily hospitalized case. It is like a negative skewed curve. On 25th day, a maximum of 180,000 people out of 18 crores are hospitalized. Here, the effect of the control $u_3(t)$ is very negligible. Fig. 8(c) shows daily death cases. It is like a negative skewed curve. On the 25th day, a maximum of 16 people out of 18 crores died. Here, also the effect of the control $u_3(t)$ is very Small. Thus, we can conclude that it is possible to control COVID-19 as long as we can reduce the reproduction number $\mathcal{R}_0 < 1$, otherwise COVID-19 will get out of control.

In Fig. 9(a), when we fully controlled, maximum of 2300000 peoples out of 18 crores are infected for reproduction number $\mathcal{R}_0 = 1.2$, where only exposed rate from Susceptible increased but other parameters are unchanged. $\mathcal{R}_0$ is estimated to determine the relative risk associated with a microbe. These estimates will be used to compare the spread of the disease with other known microbe. Without control, the number of cumulative infected case is exponentially increased with $\mathcal{R}_0$. When control is targeted to an earmarked sector, reproduction number $\mathcal{R}_0$ is not a good significance of the required control effort. Roberts and Heesterbeek are suggested a reproduction number [30]. This quantity is identical to $\mathcal{R}_0$ in the homogeneous population. In Fig. 9(b), the case of without controls and only $u_3(t)$ control, the number of deaths is increased with the increased of reproduction number $\mathcal{R}_0$. When $\mathcal{R}_0 > 1.66$, the behavior of the death curves are eccentric.

We did not include details of the results of the analysis because weights may not be very sensitive to large differences and the role of weight constant for all strategies has been explored. In Fig. 10, for different weights constants on the controls, we have shown comparative results with the implementation of strategies, and the whole pandemic situation, the value of $W_1 = 0.1$, $W_2 = 0.0007$, and $W_3 = 0.0000003$ is accurate for an optimal solution. The number of infectious cases is increased lack of implementation of interventions, in spite of the weight constants, cost of treatments and isolation efforts are increased.

6. Conclusion

For disease control and community planning for the future, optimal control is crucial. In order to eradicate the pandemic, the optimal control guides us to the parameters that we should take care of. We have formulated a mathematical model for the pandemic of COVID-19 and also discussed the transmission dynamics and control of the disease. The sensitivity of the parameters is checked in $\mathcal{R}_0$. Although the weight constants are increasing in Fig. 10, we see that number of infections and hospitalizations are also increasing in the case of under control. Infection is more likely to occur due to contact with contaminants and the prolonged life of the coronavirus. Strict lockdown, frequent hand-washing, disease side effect control, and sanitizer are the non-clinical treatment. In mild, normal, and not severe cases, recovery from COVID-19 is usually possible within fourteen days. Our research has shown that raising awareness will reduce the rapid spread of the pandemic situation. The rate of spread of the disease in each country can be explained by different precautions. According to the outcome of the investigation, we have carried out mathematical modeling work in our study which will make a big difference in terms of the number of patients if it is used carefully.

Declaration of competing interest

The authors declare that they have no known competing financial interests or personal relationships that could have appeared to influence the work reported in this paper.

References

[1] N.T. Tran, H. Tappis, N. Spilotros, S. Krause, S. Knaster, Not a luxury: a call to maintain sexual and reproductive health in humanitarian and fragile settings during the covid-19 pandemic, The Lancet Global Health 8 (6) (2020) e760–e761.

[2] J. Lourenco, R. Paton, M. Ghafari, M. Kraemer, C. Thompson, P. Simmonds, P. Klenerman, S. Gupta, Fundamental principles of epidemic spread highlight the immediate need for large-scale serological surveys to assess the stage of the sars-cov-2 epidemic, MedRxiv (2020). Pre-print.

[3] B. Cheng, Y.-M. Wang, A fundamental model and predictions for the spread of the covid-19 epidemic, MedRxiv (2020). Pre-print.

[4] Z. Cakir, H. Savas, A mathematical modelling approach in the spread of the novel 2019 coronavirus sars-cov-2 (covid-19) pandemic, 2020, electron j gen med 17 (4) (2020), em205.

[5] N.H. Tuan, H. Mohammadi, S. Rezapour, A mathematical model for covid-19 transmission by using the caputo fractional derivative, Chaos, Solitons & Fractals 140 (2020) 110107.

[6] M.M. Hasan, M. Ahmed, S.A. Urmy, Efficacy of limited antiviral treatment, testing, hospitalization, and social distancing for covid-19 pandemic, Sensors International (2021) 100112.

[7] A. Zeb, E. Alzahrani, V.S. Erturk, G. Zaman, Mathematical model for coronavirus disease 2019 (covid-19) containing isolation class, BioMed Res. Int. (2020), 2020.

[8] M. Mandal, S. Jana, S.K. Nandi, A. Khatua, S. Adak, T. Kar, A model based study on the dynamics of covid-19: prediction and control, Chaos, Solitons & Fractals 136 (2020) 109889.

[9] Y. Bai, L. Yao, T. Wei, F. Tian, D.-Y. Jin, L. Chen, M. Wang, Presumed asymptomatic carrier transmission of covid-19, Jama 323 (14) (2020) 1406–1407.

[10] A. Din, K. Shah, A. Seadawy, H. Alrabaiah, D. Baleanu, On a new conceptual mathematical model dealing the current novel coronavirus-19 infectious disease, Results in Physics 19 (2020) 103510.

[11] Kalyan Das, G. Ranjith Kumar, K. Madhusudhan Reddy, K. Lakshminarayan, Sensitivity and elasticity analysis of novel corona virus transmission model: a mathematical approach, Sensors International 2 (2021) 100088.

[12] M. Humayun Kabir, M. Osman Gani, Sajib Mandal, M. Haider Ali Biswas, Modeling the dispersal effect to reduce the infection of COVID-19 in Bangladesh, Sensors International 1 (2020) 100043.

[13] S.P. Layne, J.M. Hyman, D.M. Morens, J.K. Taubenberger, New Coronavirus Outbreak: Framing Questions for Pandemic Prevention, 2020.

[14] Amjad Salim Shaikh, Iqbal Najiroddin Shaikh, Kottakkaran Sooppy Nisar, A mathematical model of COVID-19 using fractional derivative: outbreak in India with dynamics of transmission and control, Adv. Differ. Equ. 1 (2020) 373.

[15] Aritra Ghosh, Srijita Nundy, Tapas K. Mallick, How India is dealing with COVID-19 pandemic, 2020, Sensors International (2020) 100021.

[16] D. Caccavo, Chinese and Italian covid-19 outbreaks can be correctly described by a modified sird model, medRxiv (2020). Pre-print.

[17] A. Cleo, R. Lucia, T. Athanasios, S. Constantinos, Data-based analysis, modelling and forecasting of the novel coronavirus (2019-ncov) outbreak, Medrxiv. org 2 (2020) 20.

[18] M.A. Khan, A. Atangana, Modeling the dynamics of novel coronavirus (2019-ncov) with fractional derivative, Alexandria Engineering Journal 59 (4) (2020) 2379–2389.

[19] S. Lee, G. Chowell, C. Castillo-Chavez, Optimal control of influenza pandemics: the role of antiviral treatmen and isolation, J. Theor. Biol. 265 (2010) 136–150.

[20] M. Mandal, S. Jana, S.K. Nandi, A. Khatua, S. Adak, T. Kar, A model based study on the dynamics of covid-19: prediction and control, Chaos, Solitons & Fractals 136 (2020) 109889.

[21] X. Yan, Y. Zou, Optimal and sub-optimal quarantine and isolation control in sars epidemics, Math. Comput. Model. 47 (1–2) (2008) 235–245.

[22] J.A. Martin, B.E. Hamilton, M.J. Osterman, A.K. Driscoll, Births: Final Data for 2018, 2019.

[23] C. Fraser, C.A. Donnelly, S. Cauchemez, W.P. Hanage, M.D. Van Kerkhove, T.D. Hollingsworth, J. Griffin, R.F. Baggaley, H.E. Jenkins, E.J. Lyons, et al., Pandemic potential of a strain of influenza a (H1N1): early findings, Science 324 (5934) (2009) 1557–1561.

[24] R. Nikbakht, M.R. Baneshi, A. Bahrampour, A. Hosseinnataj, Comparison of methods to estimate basic reproduction number (R_0) of influenza, using Canada 2009 and 2017-18 a (H1N1) data, J. Res. Med. Sci.: the official journal of Isfahan University of Medical Sciences 24 (2019).

[25] J.M. Heffernan, R.J. Smith, L.M. Wahl, Perspectives on the basic reproductive ratio, J. R. Soc. Interface 2 (4) (2005) 281–293.

[26] L. Pontryagin, V. Boltyanskii, R. Gamkrelidze, E. Mishchenko, The Maximum Principle, the Mathematical Theory of Optimal Processes, John Wiley and Sons, New York, 1962.

[27] G. Birkhoff, G.-C. Rota, Lecture Notes on Ordinary Differential Equations, 1960.

[28] G. Chowell, H. Nishiura, L.M. Bettencourt, Comparative estimation of the reproduction number for pandemic influenza from daily case notification data, J. R. Soc. Interface 4 (12) (2007) 155–166.

[29] A.W.-S. Ying Liu1, Albert A. Gayle, J. Rocklov, The Reproductive Number of Covid-19 Is Higher Compared to Sars Coronavirus, 2020.

[30] M. Roberts, J. Heesterbeek, A new method for estimating the effort required to control an infectious disease, Proc. Roy. Soc. Lond. B Biol. Sci. 270 (1522) (2003) 1359–1364.